Vol. 06, No. 4 (2024) 1703-1710, doi: 10.24874/PES06.04.029

Proceedings on Engineering Sciences

www.pesjournal.net

PRACTICAL INVESTIGATION OF GEOGRID-REINFORCED GRANULAR SOIL AT CYCLIC LOAD

Hassan Ali Ahmed[1]
Naser Abed Hassan
Mohammed Jassim Abed

Received 20.03.2024.
Received in revised form 17.07.2024.
Accepted 18.08.2024.
UDC – 624.159.14

Keywords:

Gravel soil, Dynamic properties, axial cumulative Strain, elasticity modulus, dynamic pore water pressure

A B S T R A C T

To examine the impact of confining pressure on the dynamic properties of geogrid-reinforced gravel soil under a similar dynamic stress ratio and dynamic stress amplitude, a dynamic triaxial test was conducted using the dynamic triaxial test apparatus. This study investigates the effect of confining pressure on the axial cumulative strain, elastic modulus, and dynamic pore pressure of reinforced gravel soil. The investigation is done under equal dynamic stress ratio and dynamic stress amplitude conditions. The findings indicate that, under equivalent dynamic stress ratios, there is a positive correlation between the increase in confining pressure and the axial cumulative strain. Conversely, the relationship is reversed when the active stress amplitude stays constant. Furthermore, increased confining pressure leads to similar values for both the elastic modulus and dynamic pore pressure. Both the modulus of elasticity and dynamic pore pressure increase when emotional stress amplitude remains constant. The damping of the elasticity modulus becomes more apparent during the initial phase of vibration, and attenuation is most evident when the confining pressure reaches 120kPa. The confining pressure significantly influences the dynamic pore pressure of reinforced gravel soil, whereas the pore pressure ratio remains unaffected. As the confining pressure increased, there was a corresponding increase in the dynamic pore pressure. Additionally, the pore pressure ratio remained relatively stable at approximately 0.6.

1. INTRODUCTION

Recently, the development of transportation infrastructures has led to roadbed diseases, such as differential settlement and degradation of bearing performance, which are caused mainly by long-term traffic dynamic loads in roadbed projects. The long-term service performance of the subgrade is substantially affected by the cumulative payments resulting from the dynamic traffic load. The challenge arises from the cumulative deformation and stiffness attenuation of the subgrade under dynamic traffic load caused by significant vibration times, low amplitude, and complex stress routes (Huang et al., 2011). Many researchers, both domestically and internationally, have conducted comprehensive experimental investigations on the

[1] Corresponding author: Hassan Ali Ahmed
Email: mr.hassanali@tu.edu.iq

dynamic properties of clay and gravel soil. These studies have yielded significant and promising outcomes. The works by Mohammed, Marwah N. et al. (2016), (2018a), (2018b), and Mohammed, Marwah Noori et al. (2019) are cited.

Erickson and Drescher (2001), the solution existed to add granular material that functions as a packing layer and distributes the loads laterally to reduce stress on the weak substrate. When dealing with complex sites, the traditional practice was to replace the unsuitable soil or to overdo it with deep foundations. Larger loads can now be supported, and failures such as settlements and narrow paving were reduced to a minimum.

Leng, J. and Gabr (2002) The characteristics of the geogrid-reinforced aggregate on soft subgrade soil were examined. Several periodic loading tests of the sheets with varied degrees of substrate thickness and kind of reinforcement were performed in a laboratory test program. The results showed that the aggregate base layer (ABC) eroded under cyclic loading, as seen by higher stresses at the Project interface as the cycle number increased. Reduced measured maximum stress (under the loaded region) and more uniformly estimated stress distribution on the subgrade soil layer are signs of stress distribution improvement caused by geosynthetic inclusion at the ABC and subgrade soil junction.

Agrawal (2011) Physical standards for separation under an asphalt access road are more complex in states. The granular stratum is pushed down and warped by the wheels of moving vehicles, depending on the weight and shape of the wheels. Because of the enlargement of gap gaps between the granular particles caused by this deformation, finer soil particles could breach the granular layer. As the vehicle travels over the granular layer more frequently, fine particles increase, and coarse aggregates collapse into the fine soil. The granular layer slowly disintegrates, making the path unavailable.

Feng et al. (2013) long-term observation data of the subgrade's dynamic response and the dynamic response of the subgrade under the influence of various loads, depths, and speeds were studied. The results suggested that the dynamic pressure of the substrate shows a decreasing trend with increasing depth, and the increasing trend of the emotional force of the substrate becomes more apparent as the vehicle load increases.

Fattah et al. (2014) focused on the model tests that also included geogrid reinforcement in the subbase layer's center and at the junction of the subgrade and subbase layer. They concluded that the reinforced sub-geogrid base's extension has a greater bearing capacity than the expansive ground soil's unreinforced substrate and the model's decreased displacement.

Indraratna et al. (2010) This study examines frequency's impact on the railway subgrade's long-term deformation. It was determined that the subgrade's constant distortion and degeneration would increase with increased frequency.

Nair and Latha (2014) Through lab examinations, researchers investigated the beneficial impacts of geosynthetic reinforcement of unpaved road subgrades. In reinforced soil-aggregate systems, a geosynthetic layer has been added at the soil-aggregate interface. The authors examined the performance of unsupported systems and other earth-supported system types to understand better the elastic and plastic strains created in the designs. Geogrids were discovered to provide a greater stress attenuation effect and to reduce plastic deformations. In contrast, reinforcing increased soil-aggregate systems' load-bearing capacity and traffic advantages.

Xiong et al. (2016) concluded that the continuous rotation of the principal stress axis caused by traffic loads would accelerate the accumulation of vertical plastic deformation and, at the same time, soften the elastic modulus.

Leng, W. et al. (2017) studied the impacts of moisture content, confining pressure and other factors on subgrade fillers' dynamic modulus and axial cumulative strain and proposed empirical formulas for dynamic elastic modulus and axial cumulative stress.

Geng et al. (2018) The effects of dynamic stress amplitude, frequency, reinforced layers, and trapped stress on the order of the dynamic modulus of elasticity of the geogrid reinforced gravel soil were investigated. The dynamic stress amplitude considerably impacted the dynamic modulus of elasticity of the reinforced soil. The reinforced substrate's bearing capacity and dynamic modulus of elasticity decrease significantly as dynamic stress increases. Frequency affects the dynamic modulus of elasticity.

Han et al. (2019) used laboratory tests to explore how the reinforcement of the geogrid affected the loose granular base. The cyclic shear test method evolved from the triaxial test procedure. The cyclic shear test showed promise in determining the impact of geogrid reinforcement, with an apparent increase in the degree of linking between geogrids and aggregates, and the triaxial tests demonstrated that the inclusion of geogrid had no effect on the elasticity modulus.

Xiao-Hua et al. (2019) the subgrade model test was conducted under the effect of one wheel for the standard axle load, and the dynamic characteristics of the low embankment were studied under vehicle load, including pavement, base, subgrade, and subsoil, in conformity with the general road design standards. As the substrate depth increases, the vertical stresses under different loading states rapidly decrease, and the stresses at flexible substrate depths vary linearly with static and short-term dynamic loads. At the same time, the strains show a non-linear trend. Since different soil layers have

different elastic modulus, the strains in the subgrade and subsoil clearly show stratification.

Wang et al. (2021) The researchers demonstrated the dynamic behavior of geogrid-reinforced gravel under cyclic sub-sinusoidal loads. It conducted large-scale triaxial cycle tests on saturated gravel soils reinforced with geogrid to investigate the effect of the number of layers of reinforcement and load frequencies on the dynamic responses of a high-speed rail track's reinforced sandy gravel substrate. The test results showed that, whereas cumulative axial stress increases with loading frequency, it reduces with reinforcing layer count. The modulus of elasticity is enhanced when there are more reinforcing layers but decreases with more frequent loading.

Researchers have investigated the dynamic properties of frequently encountered granular materials, including clay, sand, and gravel. However, there currently exists an absence of studies regarding the dynamic properties of reinforced gravel soils. The triaxial test specimens usually have widths ranging from 39 to 100 mm, whereas the loading waveforms mainly consist of sine waves. To reduce the effect of the size effect, a cylindrical sample of significant dimensions measuring (diameter is 150 mm and height is 300 mm) was chosen for testing. The dynamic characteristics of the reinforced gravel soil were considered, and a half-sine waves were used to replicate the dynamic traffic load. Subsequently, an order of cyclic loads was applied. This examination investigates the influence of confining pressure on the dynamic properties of reinforced gravel elastic modulus, and dynamic pore pressure, of reinforced gravel soil under different dynamic stress ratios (0.5, 0.75, 1.0). In addition, the influence of different confining pressures (60, 90, 120 kPa) on the dynamic properties of reinforced gravel soil was examined under the same dynamic stress ratio.

Figure 1. Plastic geogrid.

soil during a dynamic triaxial test. Specifically, the study aims to analyze the impact of confining pressure on the axial cumulative strain of reinforced gravel soil while subjecting it to the same dynamic stress ratio and dynamic stress amplitude. The relationship between the elastic modulus and dynamic pore pressure has important consequences for designing and constructing reinforced gravel soil subgrades in roadbed engineering.

2. MATERIAL AND METHOD

2.1 Materials

The study performed dynamic triaxial tests on reinforced gravel soil, investigating its dynamic under varying dynamic stress ratios and confining pressures. Figure 1 depicts a cylindrical sample of considerable size, characterized by a diameter of 150mm and a height of 300mm. The sample consists of three layers of reinforcement. The test used in this study is a consolidated undrained test, with stress control as the loading control method. The loading method utilized is single-amplitude multi-vibration loading, with a loading frequency of 1 Hz. Figure 2 shows a test that simulates the effects of traffic dynamic load. The loading waveform utilized in this test is based on the study findings of Huang et al. (2011). A half-sine wave is employed to apply cyclic dynamic load and waveform. This experiment established a comprehensive set of six working conditions, as shown in Table 1. This study investigated the variations in dynamic characteristics, including axial cumulative strain,

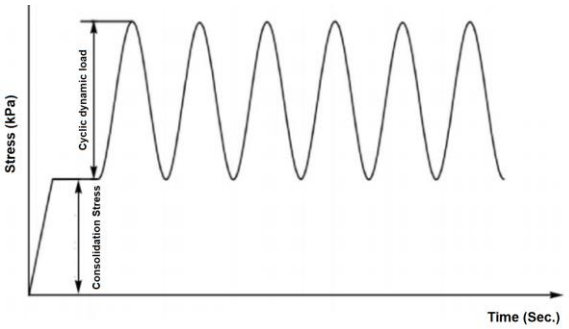

Figure 2. Schematic diagram of half-sine wave**.**

Table 1. Dynamic characteristics of six working conditions

Test sets	Confining pressure (kPa)	Dynamic stress amplitude (kPa)	Dynamic stress ratio (DSR)	Reinforcing layers
1	65	80	0.7	3
2	80	80	0.6	3
3	90	125	0.7	3
4	100	170	1.5	3
5	120	90	0.37	3
6	120	170	0.75	3

2.2 Test process

The dynamic triaxial testing of reinforcing gravel soil is used to investigate the effects of dynamic stress ratio (DSR), dynamic stress amplitude, and confining pressure on the dynamic properties of reinforced gravel soil, including axial cumulative strain, elastic modulus, and dynamic pore pressure. The dynamic stress ratio (DSR) is the dynamic stress-to-confining pressure ratio, which can reflect the dynamic stress relative to the confining pressure. Using 90 kPa as an example, the impact of different dynamic stress ratios on the dynamic properties of reinforced gravel soil, such as axial cumulative strain, elastic modulus, and dynamic pore pressure, is shown in equation 1:

$$DSR = \frac{\sigma_d}{2\sigma_3} \quad \text{..... (1)}$$

The axial dynamic stress, indicated as σ_d, and the confining pressure, indicated as σ_3, are important variables during the vibration stage. The modulus of elasticity is defined as the ratio of the dynamic stress difference (i.e., the different between the largest and lowest stress values) and the corresponding dynamic strain difference.
The correlation between the stress and strain exhibited by the restorable component of the soil is characterized as shown in equation 2:

$$E_d = \frac{\sigma_{dmax} - \sigma_{dmin}}{\varepsilon_{dmax} - \varepsilon_{dmin}} \quad \text{..... (2)}$$

Where: ($\sigma_{dmax} - \sigma_{dmin}$) is the different between the maximum and minimum values of dynamic stress; ($\varepsilon_{dmax} - \varepsilon_{dmin}$) is the difference between the maximum and minimum dynamic stress corresponding to the dynamic strain.

The test process can be roughly divided into the following steps.

1) Sample loading: adopt the mass-volume method to pack samples by layered compaction and control the quality and the number of compactions to be equal for each loading to ensure that the compaction degree of each group of models is the same.
2) The closed pressure chamber and the pressure chamber are watered.
3) Sample saturation: Use the combined head and back pressure saturation methods to saturate.
4) Sample consolidation: use isotropic consolidation;
5) Apply dynamic load: set dynamic parameters such as dynamic stress amplitude, confining pressure, frequency, etc., respectively, according to the dynamic parameters of different working conditions. The shutdown standard of this test is that the axial cumulative strain reaches 5%, or the vibration frequency reaches 5,000 times, and the test ends when one of them is satisfied. Data collection and real-time monitoring can be completed during the test through the system's software. The data collection frequency is 20 data points per second, and the sample's axial stress and strain, dynamic pore pressure, confining pressure, etc., can be recorded simultaneously.

The equipment used for the experiment is the dynamic triaxial test system. The main hardware components of the system include:

- An axial cyclic load application instrument host.
- A pressure chamber.
- A device for controlling confining pressure and pressure.
- A sensor for measuring pore pressure and load.
- A data acquisition control box.
- Computer software for data collection and control.

The maximum axial load that can be applied is 10 kN, and the maximum confining pressure and back pressure are 2 MPa. The optional frequency range is from 0.1 to 5.0 Hz and allowed waveforms include sine wave, half sine wave, and triangle wave.

3. RESULT AND DISCUSSION

The correlation between the axial cumulative strain & the vibration order at various dynamic stress ratios at a confining pressure at 90 kPa is illustrated in Figure 3. The axial cumulative strains under varied dynamic stress ratios show a consistent trend of stable development as the vibration order rises. During the initial phase of vibration, collected axial strain is rapidly developed. However, after N=1500 vibrations, the accumulated axial strain reaches a level. The link between axial cumulative strain and vibration order is examined under various dynamic stress ratios, revealing that higher dynamic stress ratios correspond to greater axial cumulative strains. The highest values of the axial cumulative strain, indicated as εd, are 2.15% and 0.75% when the dynamic stress ratios (DSR) are equal to 1.0 and 0.5, respectively. When comparing the axial cumulative strain at DSR=0.5 to that at DSR=1.0, it is observed that the rise in strain is approximately 1.96 times greater at DSR=1.0. Upon comparing the dynamic stress ratio variations, it is evident that an increase from DSR=0.5 to DSR=1.0 results in a doubling of the dynamic stress ratio. Furthermore, the axial cumulative strain experiences an approximate doubling in its amplitude. Hence, it is imperative to implement rigorous control measures on the load capacity of cars during road engineering projects to reduce the negative consequences of excessive post-construction roadbeds resulting from extended exposure to high traffic dynamic loads.

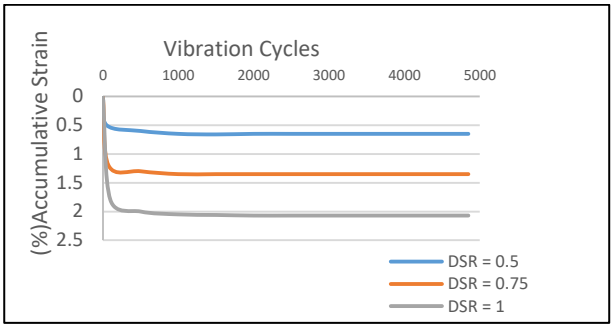

Figure 3 Shows the axial cumulative strain and vibration sequence observed under different dynamic stress ratios.

The correlation of the elastic modulus and vibration order underneath different dynamic stress ratios is seen in Figure 4. As the amount of vibration times increases, the elastic modulus has a corresponding progressive increase. However, it is seen that the elastic modulus achieves a stable state at a vibration frequency of N=1500 times. When comparing the elastic modulus under various dynamic stress ratios, the corresponding elastic modulus also increases as the dynamic stress ratio rises. However, the rate of increase in the elastic modulus decreases at higher dynamic stress ratios. The correlation between the elastic modulus and the dynamic stress ratio can be observed by analyzing the spacing of the curves in Figure 4. Specifically, when the dynamic stress ratios are 0.5 and 0.75, there is a difference of 12.20MPa between the maximum values of the elastic modulus.

Similarly, when the dynamic stress ratios are 0.75 and 1.0, the difference between the greatest elastic modulus values is 3.03MPa. The increase in the elastic modulus decreases as the dynamic stress ratio rises. The findings show that when subjected to a high dynamic stress ratio,

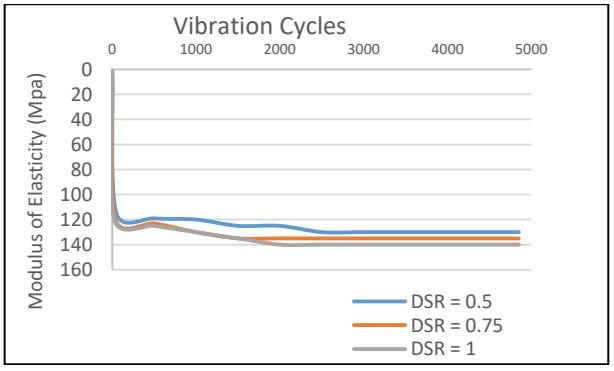

Figure 4. Illustrates how elastic modulus influences vibration order for particular dynamic stress ratios.

Figure 5 illustrates the correlation between axial cumulative strain & vibration order across various confining pressures. The relationship between axial cumulative strain and vibration order exhibits consistent patterns across different confining pressures, with the characteristics of the curve influenced by both axial cumulative strain and vibration at different dynamic stress ratios. The correlation between time and the curve shows similarities, especially during the early phase of vibration, wherein the cumulative axial strain experiences a quick escalation, followed by a sustained decline in its rate of progression.

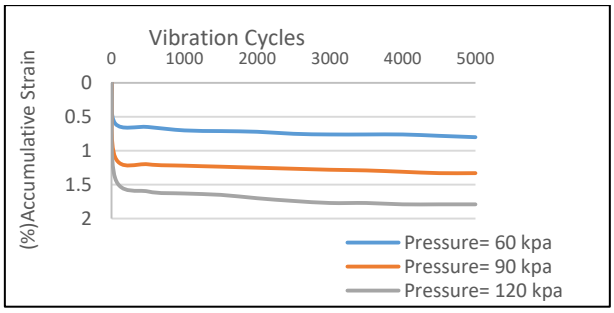

Figure 5. Shows the axial cumulative strain and vibration order at various confining pressures.

Figure 6 illustrates the correlation between the elastic modulus & vibration order across different confining pressures. During the first phase during vibration, there is an initial small fall in the elastic modulus, which is afterwards followed by a gradual and continuous increase. The curve will gradually stabilize the elastic modulus as it settles at a vibration frequency of N=1500. This phenomenon occurs due to the sudden application of axial cyclic load throughout the initial vibration stage. Consequently, the sample, formerly just subjected to consolidation confining pressure, experiences a sudden introduction of axial dynamic deviatoric stress. This sudden stress results in the change of the soil's original skeleton structure. The soil particles undergo constant motion, gradually progressing toward a heightened state of equilibrium. This phenomenon leads to changes in the stiffness of the soil, as the elastic modulus undergoes a small reduction during the early phases of vibration, followed by a gradual rise, ultimately reaching a stable condition.

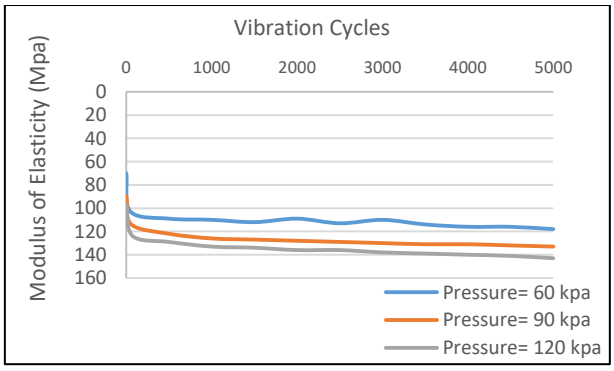

Figure 6. Shows the elastic modulus and vibration order under various confining pressures.

The relationship between dynamic pore pressure and vibration order of reinforced gravel soil under varying confining pressures is shown in Figure 7. It was seen that when the vibration frequency rises, the dynamic pore pressure experiences a rapid beginning increase. The rate of development of dynamic pore pressure shows a gradual decrease after N=200 vibration cycles, eventually achieving a stable state after N=1500 cycles. The observed pattern of pore pressure increase shows a consistent pattern indicative of suffered progression. Consequently, the dynamic stress will exhibit an upward trend when the confining pressure is increased. In addition, a combination of these two factors creates a phenomenon known as a superimposed effect, which leads to a gradual elevation in the dynamic pore pressure as the confining pressure increases. The pore pressure ratios observed under various confining pressures are shown in Table 2. Under varying confining pressures, while the maximum pore pressure increases with increased confining pressure, the pore pressure ratios do not exhibit substantial variations.

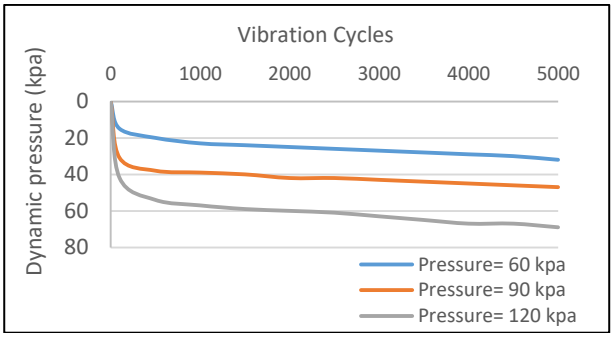

Figure 7. shows the variations in dynamic hole pressure and vibration order at a variety of confining pressures.

Table 2. presents a comparison of pore pressure ratios at a variety of confining pressures.

Confining pressure/kPa	Maximum Pore Pressure (kPa)	Pore pressure ratio
65	40	0.51
82	51	0.59
120	72	0.63

Figure 8 illustrates the correlation between the axial cumulative strain and the vibration order under certain conditions: a dynamic stress ratio (DSR) of 0.75 and a dynamic stress amplitude (A) of 80 kPa. The shapes of the curves indicating varied axial cumulative strains show similarity to the pattern observed in the order of vibrations. The axial cumulative strain exhibits a rapid increase during the initial period of vibration. When the amount of vibration exceeds a certain limit, the pace at the axial cumulative strain gradually decreases, eventually achieving a condition of equilibrium. Therefore, when subjected to similar dynamic stress ratios, the dynamic stress rises as the confining pressure increases.

Moreover, it has been noticed that the influence of these two parameters on the cumulative strain along the axis of rotation is contingent upon a specific threshold. Hence, the resultant expression typically highlights the influence of dynamic stress on the cumulative axial strain. Under an even dynamic stress ratio, the axial cumulative strain exhibits an increasing trend as the confining pressure increases.

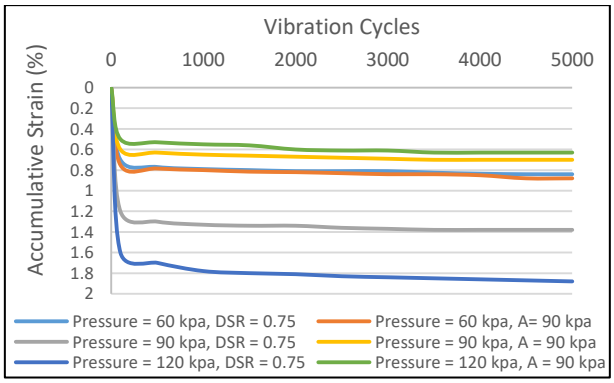

Figure 8. Axial cumulative strain & vibration sequence with the same dynamic stress ratio and amplitude

Figure 9 depicts the correlation among the elastic modulus and vibration order under specific conditions. These conditions include a dynamic stress ratio (DSR) of 0.75, a dynamic stress amplitude of 80 kPa, and variations in the dynamic stress amplitude despite a uniform DSR. The observed pattern in the development of the elastic modulus, under a constant dynamic stress ratio, is a slight reduction in the elastic modulus during the initial stage of vibration. Subsequently, a steady rise in the previously mentioned phenomenon leads to a stable state. It can be seen that, when subjected to similar dynamic stress amplitudes, the modulus of elasticity experiences a substantial initial fall during vibration, followed by a gradual increase. Eventually, the modulus achieves a stable state further impacted by increased confining pressure, resulting in the rebound effect.

The dynamic stress ratio, dynamic stress amplitude, and confining pressure show equivalents, as observed when the confining pressure reaches 60 kPa, resulting in their converging. In the reinforced gravel soil subgrade engineering field, it is essential to successfully control the relationship between confining pressure and dynamic stress by the specific engineering requirements for subgrade bearing deformations. This is necessary to ensure that the subgrade's bearing and deformation characteristics meet the imposed road operation standards when subjected to long-term traffic dynamic loads.

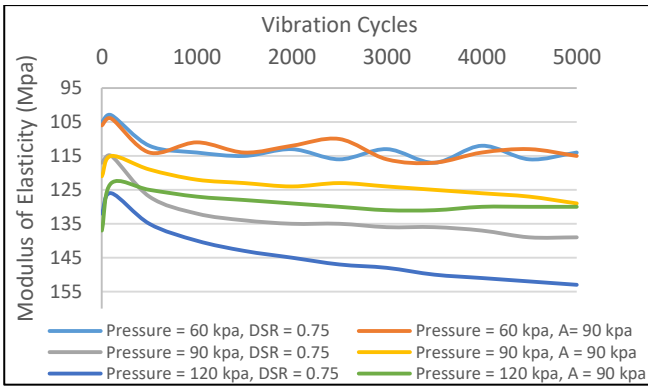

Figure 9. Elasticity modulus and vibration order under the same isokinetic stress ratio and amplitude

Figure 10 shows the relationship between dynamic pore pressure and vibration order under a dynamic stress ratio (DSR) of 0.75 and a dynamic stress amplitude of 90kPa. At the very first vibration stage, there will be an important rapid increase in the dynamic pore pressure. The sudden use of the axial cyclic load causes a sharp increase in pore pressure within the sample. Following around 200 cycles of vibration, the growth rate of dynamic pore pressure gradually diminishes. The dynamic pore pressure is maintained progressively as the vibration continues up to N=1500 cycles.

From the pore pressure ratios under different confining pressures in Table 3, it can be concluded that under other confining pressures. However, the maximum pore pressure increases with the increases of confining pressure, and the pore pressure ratios vary in different proportions.

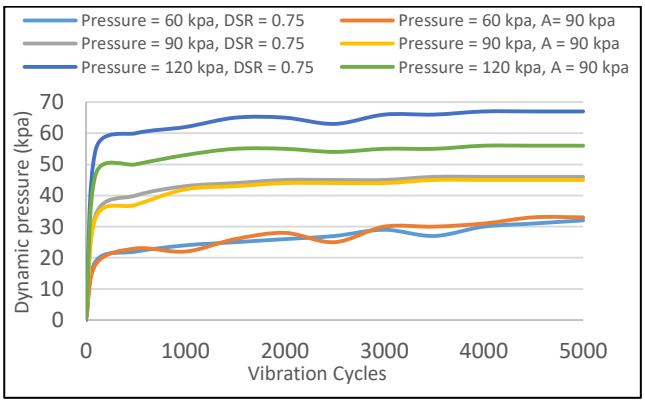

Figure 10. Dynamic pore pressure and vibration order under the same dynamic stress ratio and amplitude

Table 3. Comparison of pore pressure ratios under different confining pressures

Categories	Confining pressure/kPa	Maximum Pore Pressure/kPa	Pore pressure ratio
DSR = 0.75	65	32	0.49
	80	46	0.47
	120	67	0.57
A = 90 kpa	65	32	0.5
	80	45	0.55
	120	58	0.48

4. CONCLUSION

The dynamic triaxial test was performed on reinforced gravel soil under various dynamic stress ratios and confining pressures.

When subjected to similar confining pressure, a rise in the dynamic stress ratio results in an increase in both the axial cumulative strain and the elastic modulus. However, the effect of dynamic stress ratio changes on the dynamic hole pressure is not readily apparent. The measurements of axial cumulative strain and dynamic pore pressure show a consistent trend suggestive of a stable development pattern. In the present study, it is essential to put stringent control measures on the load bearing capacity of the vehicle to reduction the adverse effects of excessive post-construction getting off the roadbed resulting from the significant long-term traffic dynamic load.

When subjected to the same dynamic stress ratio, a rise in confining pressure leads to a corresponding rise in accumulated axial strain and the elastic modulus. However, the rate of development slightly reduction as the confining pressure rise. The dynamic pore pressure will similarly rise, and the rate of rise will also increase with the confining pressure. However, the pore pressure ratio remains approximately 0.6 at varied confining pressures, indicating that the effect of the confining pressure on the pore pressure ratio is negligible.
The elastic modulus and dynamic hole pressure are affected by applying equivalent confining pressure consistent with the same dynamic stress ratio and dynamic stress amplitude as the magnitude of the confining pressure applied to a material increases.

References

Agrawal, B. J. (2011, May). Geotextile: It's application to civil engineering–overview. *In National conference on recent trends in engineering & technology* (pp. 1-6).

Erickson, H., & Drescher, A. (2001). The use of geosynthetics to reinforce low volume roads (No. MN/RC-2001-15,).

Fattah, M. Y., Hamood, M. J., & Abbas, S. A. (2014). Behavior of plate on elastic foundation under Impact load. *Engineering and Technology Journal*, *32*(4), 1007-1027.

Feng, S. H. I., Jian-kun, L. I. U., Jian-hong, F. A. N. G., Ya-hu, T. I. A. N., & An-hua, X. U. (2013). Subgrade dynamic stress test on highway in seasonal frozen soil area. *China Journal of Highway and Transport*, *26*(5), 15.

Geng, M., Wang, D., & Li, P. (2018). Undrained dynamic behavior of reinforced subgrade under long-term cyclic loading. *Advances in Materials Science and Engineering*, *2018*.

Han, B., Ling, J., Shu, X., Song, W., Boudreau, R. L., Hu, W., & Huang, B. (2019). Quantifying the effects of geogrid reinforcement in unbound granular base. *Geotextiles and Geomembranes*, *47*(3), 369-376.

Huang Bo, Hao, D., & Yun-min, C. H. E. N. (2011). Simulation of high-speed train load by dynamic triaxial tests. *Chinese Journal of Geotechnical Engineering*, *33*(2), 195.

Indraratna, B., Thakur, P. K., & Vinod, J. S. (2010). Experimental and numerical study of railway ballast behavior under cyclic loading. *International Journal of Geomechanics*, *10*(4), 136-144.

Leng, J., & Gabr, M. A. (2002). Characteristics of geogrid-reinforced aggregate under cyclic load. *Transportation research record*, *1786*(1), 29-35.

Leng, W., Xiao, Y., Nie, R., Zhou, W., & Liu, W. (2017). Investigating strength and deformation characteristics of heavy-haul railway embankment materials using large-scale undrained cyclic triaxial tests. *International Journal of Geomechanics*, *17*(9), 04017074.

Mohammed, M. N., Yusoh, K. B., & Shariffuddin, J. H. B. H. (2016). Methodized depiction of design of experiment for parameters optimization in synthesis of poly (Nvinylcaprolactam) thermoresponsive polymers. *Materials Research Express*, *3*(12), 125302.

Mohammed, M. N., Yusoh, K. B., & Shariffuddin, J. H. B. H. (2018). Parametric Optimization of the Poly (Nvinylcaprolactam)(PNVCL) Thermoresponsive Polymers Synthesis by the Response Surface Methodology and Radial Basis Function neural network. *In MATEC Web of Conferences* (Vol. 225, p. 02023*). EDP Sciences.*

Mohammed, M. N., Yusoh, K. B., & Shariffuddin, J. H. B. H. (2018). Poly (N-vinyl caprolactam) thermoresponsive polymer in novel drug delivery systems: A review. *Materials Express*, *8*(1), 21-34.

Mohammed, M. N., Yusoh, K. B., Ismael, M. N., & Shariffuddin, J. H. B. H. (2019). Synthesis of thermo-responsive poly (N-vinylcaprolactam): RSM-based parameters optimization. Multiscale and Multidisciplinary Modeling, *Experiments and Design*, *2*, 199-207.

Nair, A. M., & Latha, G. M. (2014). Cyclic loading behaviour of reinforced soil–aggregate bases. *Proceedings of the Institution of Civil Engineers-Ground Improvement*, *167*(2), 88-98.

Wang, J. Q., Chang, Z. C., Xue, J. F., Lin, Z. N., & Tang, Y. (2021). Experimental Investigation on the Behavior of Gravelly Sand Reinforced with Geogrid under Cyclic Loading. *Applied Sciences*, *11*(24), 12152.

Xiao-hua, YANG, Qi, WAN, Da-peng, LIU and Han, BAO. (2019). Dynamic characteristics of gravel soil low embankment in Xinjiang. *Journal of Transportation Engineering*, *19*(3),1-9.

Hassan Ali Ahmed
College of Engineering,
Tikrit University,
Tikrit,
Iraq
mr.hassanali@tu.edu.iq
ORCID 0000-0001-9532-024X

Naser Abed Hassan
College of Engineering,
Tikrit University,
Tikrit,
Iraq
naser.a.hassan@tu.edu.iq
ORCID 0000-0003-2768-7124

Mohammed Jassim Abed
College of Engineering,
Tikrit University,
Tikrit,
Iraq
eng.mja@tu.edu.iq
ORCID 0000-0002-0259-9809